Title: IGF-I prevents HIF-1α-dependent G1/S arrest by activating cyclin E/CDK2 via the PI3K/AKT/FOXO1/Cdkn1b pathway in porcine granulosa cells

Running title: IGF-I restores G1/S transition in hypoxic GCs

Summary sentence: The IGF-I/PI3K/AKT/FOXO1/Cdkn1b axis is essential for preserving G1/S progression in hypoxic porcine GCs by targeting cyclin E/CDK2

Chengyu Li[a], Zhaojun Liu[a], Jiaqi Zhou[a], Xueqin Meng[a], Shuo Liu[a], Weijian Li[a], Xue Zhang[a], Jilong Zhou[b], Wang Yao[a], Chao Dong[a], Yan Cao[a], Rongyang Li[a], Baobao Chen[a], Aiwen Jiang[a], Yi Jiang[a], Caibo Ning[a], Fang Zhao[a], Yinghui Wei[a], Shao-chen Sun[a], Jingli Tao[a], Wangjun Wu[a], Ming Shen[a,]*, Honglin Liu[a,]*

[a]College of Animal Science and Technology, Nanjing Agricultural University, Nanjing 210095, China

[b]Institute of Stem Cell and Regenerative Biology, College of Animal Science and Veterinary Medicine, Huazhong Agricultural University, Wuhan, 430070, China

*Correspondence author:

1. Ming Shen, College of Animal Science and Technology, Nanjing Agricultural University, Weigang 1, Nanjing, 210095, China. Tel: 13585117208; E-mail: shenm2015@njau.edu.cn

2. Honglin Liu, College of Animal Science and Technology, Nanjing Agricultural University, Weigang 1, Nanjing, 210095, China. Tel/Fax: 86-25-84395106; E-mail: liuhonglin@njau.edu.cn

Abstract

As the follicle develops, the thickening of the granulosa compartment leads to progressively deficient supply of oxygen in GCs due to the growing distances from the follicular vessels. These conditions are believed to cause hypoxia in GCs during folliculogenesis. Upon hypoxic conditions, several types of mammalian cells have been reported to undergo cell cycle arrest. However, it remains unclear whether hypoxia exerts any impact on cell cycle progression of GCs. On the other hand, although the GCs may live in a hypoxic environment, their mitotic capability appears to be unaffected in growing follicles. It thus raises the question whether there are certain intra-ovarian factors that might overcome the inhibitory effects of hypoxia. The present study provides the first evidence suggesting that $CoCl_2$-mimicked hypoxia prevented G1-to-S cell cycle progression in porcine GCs. In addition, we demonstrated that the inhibitory effects of $CoCl_2$ on GCs cell cycle are mediated through HIF-1α/FOXO1/Cdkn1b pathway. Moreover, we identified IGF-I as an intra-follicular factor required for cell cycle recovery by binding to IGFR in GCs suffering $CoCl_2$ stimulation. Further investigations confirmed a role of IGF-I in preserving G1/S progression of $CoCl_2$-treated GCs via activating the cyclin E/CDK2 complex through the PI3K/AKT/FOXO1/Cdkn1b axis. Although the present findings were based on a hypoxia mimicking model by using $CoCl_2$, our study might shed new light on the regulatory mechanism of GCs cell cycle upon hypoxic stimulation.

Key words: hypoxic stimulation / IGF-I / HIF-1α / cell cycle / G1/S arrest / porcine

granulosa cells

1. Introduction

In mammalian ovaries, follicular angiogenesis is restricted to the theca interna layer, while the granulosa cells (GCs) and oocytes develop in an environment without blood vessels [1]. The vascularized and non-vascularized follicle compartment is separated by the basement membrane, which prevents the follicular vasculature from penetrating into the granulosa layer throughout folliculogenesis [2, 3]. As the follicle develops, the proliferation of GCs and thickening of the granulosa compartment might lead to progressively deficient supply of oxygen and nutrients in GCs due to the growing distances from the follicular vessels [2-4]. These conditions seem to cause hypoxia in GCs during folliculogenesis. In fact, it has been suggested that the ovarian follicles have structural similarity to a tumor, because both of them were presumed to contain a hypoxic core [5, 6]. As a result of steadily increasing cell density in the GCs layers, the decreased O_2 levels (the O_2 level was modeled rather than actually measured) [7] trigger a hypoxic response that was also found in other tumor cells enduring low oxygen tension [8].

One of the decisive elements involved in the physiological responses to hypoxia is the hypoxia-inducible factor 1 (HIF-1) [9]. HIF-1 is a heterodimeric protein consistsing of a oxygen-sensitive α subunit and a constitutively expressed β subunit [10]. In normoxia conditions, HIF-1α undergoing post-translational modifications (including hydroxylation and ubiquitination) is rapidly degraded by the ubiquitin–proteasome pathway [11-13]. Upon hypoxic exposure, the stabilization of HIF-1α results in activation of the HIF-1 transcription

factor complex that regulates expression of genes required for angiogenesis, glycolysis, and cell survival [14]. In the ovary, HIF-1α expression was detected in GCs of preantral, antral, and preovulatory follicles [15]. Moreover, emerging evidence indicates a role for HIF-1α in follicular development and ovulation [16].

Hypoxia has been suggested to alter cell cycle progression[17]. There are studies which have reported that hypoxia is responsible for cell cycle arrest in G0/G1 and blocked G1/S transitions [18, 19]. Several lines of research have indicated that hypoxia-induced cell cycle arrest is associated with a decreased activity of certain cyclin-CDK complexes [18, 20]. Although these studies revealed an down-regulation of cyclin-CDK components, such as CDK4, and cyclin D, cyclin E, and an up-regulation of cyclin-dependent kinase inhibitors, such as Cdkn1b, most of the data were obtained from experiments using transformed or immortalized cells where the cell cycle machinery has already been manipulated [21, 22]. On the other hand, although a recent study on bovine GCs revealed a G0/G1 arrest induced by low oxygen exposure [23], there are no reports of cell cycle regulation in response to hypoxic stress in porcine ovarian GCs. Several groups have shown that the hypoxic induction of cell cycle arrest is dependent on HIF-1α, a proxy for resumed hypoxia [17]. However, it remains unclear whether HIF-1α is relevant to GCs cell cycle regulation in developing porcine follicles.

Insulin-like growth factor-I (IGF-I) is a polypeptide hormone that play essential roles in stimulating mammalian ovarian follicular development [24]. In vivo studies indicate that IGF-I is highly expressed in the actively growing follicles of rats [25]. From the beginning in the early postpartum period [25], concentrations of IGF-I in follicular fluid increase with

increased follicular size in gilts [26]. In rat growing follicles, the expression of IGF-I is selectively confined to GCs [25, 27], where the IGF-I receptor is also concentrated [25, 28]. IGF-I is well recognized for its ability to promote proliferation as well as survival in several types of cells including GCs [29]. For example, IGF-I has been shown to induce mitosis of mouse ovarian GCs cultured in vitro [30]. In contrast, GCs proliferation is blocked in the ovary of *Igf1* null mice [31]. However, current evidence does not indicate a direct action of IGF-I on hypoxia-induced cell cycle arrest of porcine GCs.

FOXO1, a member of the forkhead box O (FOXO) family, plays essential roles in diverse cellular and physiological processes [32]. Previous studies demonstrated that insulin or IGF-I increased FOXO1 phosphorylation via activation of phoshatidylinositol-3 kinase (PI3K)/AKT signaling [32]. In the presence of insulin and/or growth factors, PI3K activates AKT through phosphorylation, and active AKT, in turn, inhibits the transcriptional activation of FOXO1 via phosphorylation-dependent nuclear exclusion [32]. FOXO1 has been reported to inhibit cell cycle progression by inducing expression of some CDK inhibitors including Cdkn1b [33]. However, little is known regarding whether the PI3K/AKT/FOXO1 pathway plays a role in the cell cycle regulation of GCs in response to hypoxia stimulation.

In this study, we documented that $CoCl_2$-mimicked hypoxic stimulation impairs the G1/S cell cycle transition of porcine GCs by increasing HIF-1α accumulation, which compromises cyclin E/CDK2 activity through FOXO1-dependent induction of Cdkn1b function. In addition, we identified IGF-I as a potential intra-ovarian factor required for maintaining GCs cell cycle progression upon hypoxic exposure by activating the PI3K/AKT/FOXO1/Cdkn1b axis, which in turn release cyclin E/CDK2 complex from

Cdkn1b-mediated inhibition, and thus restoring the G1/S transition of porcine GCs.

2. Material and Methods

2.1 Reagents and antibodies

PX-478 (S7612), AS1842856 (S8222), H89 (S1582), LY294002 (S1105), Go6983 (S2911), SCH772984 (S7101), and GSK1904529A (S1093) were purchased from Selleck Chemicals (Houston, TX, USA). Antibodies against HIF-1α (Cat.No. 14179; Lot.No. 1), mTOR (mTORC1, Cat.No. 2983; Lot.No. 16), p-mTOR (Cat.No. 5536; Lot.No. 7), α-Tublin (Cat.No. 2125; Lot.No. 11), Cdkn1b (Cat.No. 3686; Lot.No. 5), FOXO1 (Cat.No. 2880; Lot.No. 11), p-FOXO1 (Cat.No. 9461; Lot.No. 9), AKT (Cat.No. 9272; Lot.No. 17), and p-AKT (Cat.No. 4060; Lot.No. 16) were obtained from Cell Signaling Technology (Beverly, MA, USA). Antibodies against cyclin E (Cat.No. A14225; Lot.No. 0212390301), cyclin D1 (Cat.No. A11022; Lot.No. 1154390201), CDK6 (Cat.No. A0705; Lot.No. 1000870201), CDK4 (Cat.No. A0366; Lot.No. 0074920201), and CDK2 (Cat.No. A0294; Lot.No. 3560007104) were purchased from ABclone (Woburn, MA, USA). Human LR3 IGF-1/IGF-I/IGF-1 Protein (10598-HNAY1) was bought from Sino Biological (Beijing, China).

2.2 Sample collection, cell culture and treatments

Porcine ovaries collected from 1200 mature sows at a local slaughterhouse (Changzhou Erhualian Pig Production Cooperation, Jiangsu, China) were transferred to the laboratory within 2 h in 0.9% saline maintained at 37℃, washed six times with 0.9% sterilized NaCl solution plus gentamicin sulfate (1:400) (Kelong Veterinary Drugs Co., Shanxi, China), and

GCs (a mixture of cumulus granulosa cells and mural granulosa cells) were then obtained from 3-5 mm antral follicles by aspiration using a syringe with a 20-gauge needle. After washing with PBS (Gibco; 1 mM KH_2PO_4, 155 mM NaCl, 3 mM Na_2HPO_4-$7H_2O$), cells were centrifuged at 1000 g for 5 min, and immediately seeded into 6-wells plates at a density of 5×10^5/ml, and grown in DMEM/F-12 (1:1) medium (Gibco) containing 10% fetal bovine serum (FBS; Sigma), 100 units/ml penicillin, and 100 μg/ml streptomycin (Gibco) for 2 days at 37℃ with 5% CO_2. For drug administration, GCs were incubated with/without 100 μM $CoCl_2$ (Sigma) in the presence or absence of IGF-I (30 ng/ml) for 6 h or 24 h. In some experiments, cells were treated with the HIF-1α inhibitor PX-478 (2 μM), FOXO1 inhibitor AS1842856 (500 nM), IGF-I receptor (IGFR) inhibitor GSK1904529A (5 μM), PKA inhibitor H89 (5 μM), PI3K/AKT inhibitor LY294002 (10 μM), PKC inhibitor Go6983 (5 μM), or ERK1/2 inhibitor SCH772984 (5 μM) for 2 h before $CoCl_2$ incubation.

2.3 Flow Cytometry

GCs received desired treatments were digested in 0.25% trypsin (Gibco), rinsed with cold PBS (Gibco; 1 mM KH_2PO_4, 155 mM NaCl, 3 mM Na_2HPO_4-$7H_2O$), and fixed with 70% ethanol for 2 h. After washing with PBS (Gibco; 1 mM KH_2PO_4, 155 mM NaCl, 3 mM Na_2HPO_4-$7H_2O$), cells were incubated with the propidium iodide (PI)/RNase A staining solution (Rnase A:PI=9:1; KeyGEN) for 30-60 min at 4℃ in the dark. Cell cycle assay was then performed using a BD Accuri C6 flow cytometer (Becton Dickinson).

2.4 cyclin E/CDK2 activity assay

The activity of cyclin E/CDK2 complex was determined using a GENMED cyclin E/CDK2 activity detection kit (GMS50147, GENMED , Shanghai, China). This colorimetric strategy is based on CDK1-mediated phosphorylation of Ser in target sequence HHASPRK, which in turn promotes the conversion of NADH into NAD+ via the pyruvate kinase/lactate dehydrogenase reaction system. The alterations of optical density at 340 nm were analyzed to quantify the specific activity of cyclin E/CDK2. Briefly, GCs cultured in 100 mm petri dish were grown to a total number of 1×10^7, washed with GENMED cleaning solution (Reagent A), gently scraped off the cells using a cell scraper. After centrifugation at 300 g (4℃) for 5 min, GENMED lysis buffer (Reagent B) were added into the cell pellets, and incubated on ice for 30 min. The cytosolic extracts were centrifuged at 16,000 g at 4℃ for 5 min, and protein concentrations were determined using a Bradford Protein Assay Kit (P0006, Beyotime Institute of Biotechnology, Shanghai, China). A total of 100 μg of protein was incubated with 10 μL chromophoric substrate at 37℃. The optical density of each sample was immediately determined at 340 nm under a microplate spectrophotometer (Thermo Fisher Scientific, Camarillo, CA, USA).

2.5 Immunofluorescent and confocal microscopy

GCs seeded on coverslips (10×10 mm^2) at a density of 5×10^5/ml were grown to approximately 70% confluence, subjected to the desired treatment, and then fixed using 4% paraformaldehyde (PFA) for 1 h at room temperature. Cells were washed three times in PBS (Gibco; 1 mM KH_2PO_4, 155 mM NaCl, 3 mM Na_2HPO_4-$7H_2O$), and then permeabilized with 0.5% Triton X-100 (Sigma-Aldrich, T8787) for 10 min at 4 ℃. After blocking with 1% BSA

(Sigma-Aldrich, A3059) for 1 h at room temperature, GCs were incubated with anti-FOXO1 (1:100) antibody or anti-HIF-1α (1:100) antibody for 1 h at 37 ℃, followed by incubation with an Alexa Fluor 488-conjugated secondary antibody (1:200; excitation wavelength: 488 nm; emission wavelength: 520 nm) for 1 h, and the nuclei were counterstained with DAPI (excitation wavelength: 358 nm; emission wavelength: 461 nm) for 10 min at room temperature. Fluorescent images were captured using a laser-scanning confocal fluorescent microscope (Carl Zeiss, Oberkochen, Germany).

2.6 Western blot

Equal amounts of proteins extracted from cultured GCs using radioimmune precipitation assay buffer (Beyotime Institute of Biotechnology, Shanghai, China) were fractioned by electrophoresis on a 4-20 % Sure PAGE gel (Genscript, Nanjing, China) and transferred to PVDF membranes (Millipore, Bedford, MA) by electroblotting. Nonspecific binding sites were blocked with TBST (Solarbio) containing 5% bovine serum albumin. The membranes were then treated with primary antibodies (1:1000) in blocking solution overnight at 4℃. After washing in TBST three times, the membranes were incubated with an appropriate secondary antibody (1:2000) at room temperature for 2 h. Signal detection was performed using WesternBright ECL HRP substrate kit (Advansta) under a LAS-4000 luminescent image analyzer (Fuji Film Co., Ltd., Tokyo, Japan). Bands were quantified with ImageJ 1.42q software. The relative expression of target proteins was normalized to TUBA1A as the loading control.

2.7 Immunoprecipitation assay

GCs washed with PBS (Gibco; 1 mM KH_2PO_4, 155 mM NaCl, 3 mM Na_2HPO_4-$7H_2O$) were lysed on ice using IP lysis buffer (Beyotime Institute of Biotechnology, Shanghai, China) containing protease inhibitor cocktail (Roche, Mannheim, Germany). Whole-cell lysates (WCL) were subjected to immunoprecipitation with anti-Cdkn1b antibody. We added 5 μL of antibody to 500 μL of cell lysate to reach a final concentration at 20 ng/μL. The mixture was then incubated at 4℃ overnight. After addition of 25 μL Protein A/G Magnetic Beads (88802, Thermo Scientific, San Jose, CA), the mixture were incubated with gentle rocking for 1 h at 4 ℃. Pellet beads using magnetic force and discard the supernatant. The pellets were washed using 1×cell lysis buffer, magnetized again to remove the supernatant, resuspended with 1×SDS loading buffer (SunShineBio, Nanjing, China), and then processed for western blotting with the indicated antibodies.

2.8 Statistical analysis

Statistical analyses were performed using the SPSS software version 20.0 (SPSS). Data were presented as mean ± SEM of at least three independent experiments. Differences between two groups were assessed using the Student t-test, and between multiple groups using one-way ANOVA, followed by LSD post hoc test. At least three technical repeats were included in each experiment. P-values less than 0.05 were considered significant.

3. Results

3.1 $CoCl_2$-induced hypoxia causes a cell cycle arrest in porcine GCs

Cobalt chloride ($CoCl_2$) has been widely used as a hypoxia-mimicking agent in both in vivo and in vitro studies [34, 35]. $CoCl_2$ simulates hypoxia, at least in part, by inhibiting the hydroxylation of HIF-1α, thus preventing it from pVHL-mediated degradation [36]. $CoCl_2$ has also been shown to activate downstream signaling pathways of hypoxic stress [37]. To examine whether $CoCl_2$ exposure induces hypoxic response in vitro, primary cultured porcine GCs were treated with the indicated concentration of $CoCl_2$ for 0, 2, 4, 6, or 12 h, and then collected for western blotting using an antibody against the hypoxia marker HIF-1α. As shown in Fig 1A, the protein level of HIF-1α was significantly increased after $CoCl_2$ treatment. This suggested that the hypoxia-mimetic agent $CoCl_2$ successfully stimulated the hypoxic response in porcine GCs.

We next tested the effect of $CoCl_2$ on the cell cycle progression of GCs. As shown in Fig 1B, treatment with $CoCl_2$ significantly increased the percentage of cells in G0/G1 phases, but reduced the population in S phase, indicating an impaired G1/S transition. Both western blot analysis and immunofluorescence staining results showed that, compared with control cells, expression of protein for the cyclin-dependent kinase (CDK) inhibitor Cdkn1b was markedly increased after 24 h of $CoCl_2$ exposure (Fig 1C and D). Correspondingly, decreased activity of the cyclin E/CDK2 complex was detected after $CoCl_2$ incubation (Fig 1E). These data clearly suggested that GCs respond to $CoCl_2$-mimicked hypoxia through a compromised progression from G0/G1 to S phase.

3.2 $CoCl_2$-mimicked Hypoxic stimulation of HIF-1α prevents porcine GCs from G1/S transition

To determine whether it is HIF-1α, rather than other hypoxic effects, that induces cell cycle arrest, we used PX-478, a HIF-1α antagonist that was reported to suppress HIF-1α at both transcriptional and translational levels [38], to restrain HIF-1α activity and examined GCs cell cycle by flow cytometry. As shown in Fig 2A and B, the proportion of G1/S-arrested cells upon $CoCl_2$ exposure was significantly reduced in GCs received 2 μM PX-478 administration, thus PX-478 concentration at 2 μM were selected for our subsequent experiments. The results suggested that HIF-1α is responsible for the inhibition of GCs cell cycle under $CoCl_2$-mimicked hypoxic conditions. Consistent with this, the blocking of HIF-1α function repressed the $CoCl_2$-induced up-regulation of Cdkn1b (Fig 2C and D), which was associated with a recovery of cyclin E/CDK2 activity (Fig 2E). However, no significant change in the levels of cyclin D1, cyclin E, CDK2, CDK4, and CDK6 was observed after inhibiting HIF-1α in $CoCl_2$-treated porcine GCs (Fig 2C).

3.3 Inhibition of cyclin E/CDK2 activity through the HIF-1α/FoxO1/Cdkn1b axis is required for the induction of G1/S arrest

It has been documented that FOXO1 is involved in cell cycle regulation by targeting some CDK inhibitors including Cdkn1b [33]. We thus examined whether FOXO1 is correlated with $CoCl_2$-mediated G1/S arrest in cultured porcine GCs. As reported, the specific functions of FOXO1 are achieved by post-translational modifications and subcellular localization. In particular, phosphorylation of FOXO1 by PI3K/AKT results in the exportation of FOXO1 from the nucleus and thus inhibiting FOXO1-dependent transcription [39]. In contrast, AKT suppression induces dephosphorylation and nuclear distribution of FOXO1 [39]. As shown in

Fig 3A, $CoCl_2$ incubation increased the expression of total FOXO1 and led to its dephosphorylation at Ser256 (In this study, p-FOXO1 refers to phosphorylation of FOXO1 at Ser256). In accordance with this, AKT, a major inhibitory kinase of FOXO1, displayed decreased activity (as suggested by decreased phosphorylation of AKT) following $CoCl_2$ treatment (Fig 3B). Accordingly, the phosphorylation of mTOR, a downstream effector and indicator of AKT activity [40], was also reduced in $CoCl_2$-treated GCs, further confirmed the inhibitory effects of $CoCl_2$ on AKT activity. Notably, the induction of FOXO1 (as reflected by increased expression and decreased phosphorylation) was blocked after inhibiting HIF-1α with PX-478, which also abolished the dephosphorylation of AKT upon $CoCl_2$ stimulation (Fig 3C), suggesting that $CoCl_2$ might depress the p-AKT/p-FOXO1 pathway through a HIF-1α dependent manner. We next determined the subcellular localization of FOXO1 upon $CoCl_2$ stimulation. As shown in Fig 4A, compared with the control group, the nuclear distribution of FOXO1 was significantly increased in porcine GCs after treatment with $CoCl_2$ for 6 h. To test whether FOXO1 is required for $CoCl_2$-induced Cdkn1b expression, GCs were treated with AS1842856, an inhibitor that blocks the transcription activity of FOXO1. The results in Fig 4B and C showed that the $CoCl_2$-upregulated expression of Cdkn1b was significantly decreased in GCs treated with the FOXO1 inhibitor. On the other hand, inactivation of FOXO1 provided no obvious inhibitory effects on the expression levels of p-AKT (Ser473) during $CoCl_2$ exposure (Fig 4B).

Since Cdkn1b has been reported as a repressor of G1/S progression by interacting with the cyclin E/CDK2 complex and blocking its activity [41], we wonder whether $CoCl_2$-induced activation of FOXO1/Cdkn1b pathway affects the binding status between

Cdkn1b and cyclin E/CDK2 in GCs suffering $CoCl_2$ exposure. To test this assumption, GCs exposed to $CoCl_2$ incubation were collected for immunoprecipitation with the antibody against Cdkn1b. As shown in Fig 4D, both cyclin E and CDK2 were coprecipitated by the Cdkn1b antibody. Upon $CoCl_2$ treatment, the binding affinity of Cdkn1b to cyclin E/CDK2 was markedly increased, implying an enhanced physical interaction between Cdkn1b and cyclin E/CDK2 under $CoCl_2$-mimicked hypoxic conditions. In accordance with this, compared with the control cells, significantly lower activity of the cyclin E/CDK2 complex was detected in GCs treated with $CoCl_2$ (Fig 1E). Moreover, the inhibition of both HIF-1α and FOXO1 partly reduced the association between Cdkn1b and cyclin E/CDK2 complex upon $CoCl_2$ exposure, but the FOXO1 inhibitor failed to further repress Cdkn1b-cyclin E/CDK2 interaction in cells pretreated with PX-478 (Fig 4E). Correspondingly, antagonists against HIF-1α and/or FOXO1 restored cell cycle progression in $CoCl_2$-treated GCs (Fig 4F and Supplementary Figure 1). However, inhibition of FOXO1 provided no additional effects on facilitating G1-to-S phase progression in PX-478-treated cells (Fig 4F). Consistent results were obtained by determining cyclin E/CDK2 activity of GCs (Fig 4G), further confirming that the deactivation of cyclin E/CDK2 complex through the HIF-1α/FOXO1/Cdkn1b pathway might be an essential step in $CoCl_2$-mediated suppression of G1/S transition in porcine GCs.

3.4 IGF-I restores G1/S transition in $CoCl_2$-treated porcine GCs

Follicular growth is accompanied by the proliferation of GCs. Since the multiplication of the GCs does not spontaneously stop in larger follicles, which tended to have lower levels of

oxygen partial pressure (pO2) [5], we suspected that certain intra-ovarian factors might overcome the inhibitory effects of hypoxia on GCs cell cycle in vivo. To identify the factors that prevent GCs from hypoxia-induced G1/S arrest, we examined the possible effects of FSH, E2, and IGF-I, all of which have been implicated in the regulation of GCs proliferation during follicular development [42, 43]. As shown in Supplementary Figure 2, FSH, LH, and E2 failed to activate G1/S transition when GCs were exposed to $CoCl_2$. In contrast IGF-I remarkably reduced the proportion of G1/S-arrested cells (Fig 5A-D). Accordingly, GCs with IGF-I treatment showed a significant restoration of cyclin E/CDK2 activity upon $CoCl_2$-mimicked hypoxic stimulation (Fig 5E).

In GCs, IGF-I-mediated effects are achieved via its binding to the IGF-I receptor (IGF-IR) [25, 27, 28]. To determine whether the recovery of G1/S transition by IGF-I is an IGF-IR-dependent event, we treated cells with GSK1904529A, a specific antagonist of IGF-IR. As shown in Supplementary Figure 3, GSK1904529A abrogated IGF-I-induced G1/S transition in GCs received $CoCl_2$ administration. Based on these data, we proposed that IGF-I might be essential for maintaining cell cycle progression of porcine GCs during $CoCl_2$ stimulation.

3.5 IGF-I overcomes $CoCl_2$-induced G1/S arrest via activating the PI3K/AKT signaling

IGF-I has been suggested to activate multiple downstream signaling cascades in GCs, including PKA, PI3K, AKT, PKC, and ERK1/2 [30, 44, 45]. To test whether these pathways might be involved in IGF-I-mediated cell cycle regulation in GCs, we performed flow cytometric assay. As shown in Fig 6A-D and Supplementary Figure 4, blocking PI3K/AKT

with LY294002 restored $CoCl_2$-induced G1/S arrest in the presence of IGF-I, whereas inhibitors against PKA (H89), PKC (Go6983), or ERK1/2 (SCH772984) had no effect. Consistent results were observed by determining cyclin E/CDK2 activity, which showed a significant decline in IGF-I-treated GCs following the inhibition of PI3K/AKT, rather than PKA, PKC, or ERK1/2 (Fig 6E-H). These data indicated that the PI3K/AKT pathway might be involved in IGF-I-mediated resumption of G1/S transition in porcine GCs in the presence of a signal for hypoxia.

3.6 The effects of IGF-I are mediated by activating cyclin E/CDK2 through the PI3K/AKT/FOXO1/Cdkn1b axis

To further probe the IGF-I signaling, we determined the activation of AKT, FOXO1, and HIF-1α. As shown in Fig 7A, IGF-I markedly inhibited $CoCl_2$-induced dephosphorylation of both AKT and FOXO1, but did not influence the accumulation of HIF-1α. Immunofluorescence staining indicated that the nuclear localization of FOXO1 upon $CoCl_2$ stimulation was blocked after IGF-I treatment (Fig 7B and Supplementary Figure 5A). By contrast, the PI3K/AKT inhibitor LY294002 restored $CoCl_2$-induced nuclear transportation of FOXO1 in GCs despite IGF-I administration (Fig 7B and Supplementary Figure 5A). Consistently, the actions of IGF-I in suppressing $CoCl_2$-upregulated Cdkn1b expression were reversed by inhibiting the PI3K/AKT pathway (Fig 7C, Supplementary Figure 5B, and Fig 7D). These data suggested that the $CoCl_2$-triggered induction of FOXO1/Cdkn1b pathway was suppressed by IGF-I through the PI3K/AKT signaling.

We next tested whether the PI3K/AKT/FOXO1/Cdkn1b axis is correlated with

IGF-I-mediated cell cycle recovery upon $CoCl_2$ stimulation. Using immunoprecipitation, we found that IGF-I significantly repressed Cdkn1b-cyclin E/CDK2 interaction following $CoCl_2$ incubation (Fig 7E). Corresponding, IGF-I reversed the inhibition of cyclin E/CDK2 activity by $CoCl_2$ (Fig 5E). Conversely, the inhibition of PI3K/AKT restored the association between Cdkn1b and cyclin E/CDK2 (Fig 7E), which was accompanied by an impaired cyclin E/CDK2 activity in GCs with IGF-I treatment (Fig 7F). However, the inhibitory effects of Cdkn1b on cyclin E/CDK2 were abolished after repressing FOXO1 in LY294002-treated GCs (Fig 7F and G). Accordingly, inhibition of FOXO1 in GCs with IGF-I treatment induced G1-to-S phase progression despite LY294002 administration. (Fig 7H and I), which further confirmed the role of IGF-I/PI3K/AKT/FOXO1/Cdkn1b signaling in restoring G1/S transition of porcine GCs under $CoCl_2$-mimicked hypoxic conditions.

4. Discussion

The proliferation of GCs is critical for follicular development and ovulation [46]. However, in normally growing follicles, the enlargement of the GCs compartment is supposed to cause progressively more hypoxic conditions [2-4]. Hypoxia has been demonstrated to inhibit cell cycle progression in rapidly proliferating mammalian cells [18, 19]. Since hypoxia occurs concomitantly with GCs multiplication during follicular growth, it raises the question whether hypoxia exerts any impact on cell cycle progression of GCs.

To investigate the correlation between hypoxia and GCs cell cycle, we performed experiments in porcine GCs. Our current findings showed that the hypoxic stimulation induces an accumulation of GCs in G0/G1. We also observed a decreased population of S

phase in cells that displayed G0/G1 arrest. Although a possible G2/M delay has been reported in some hypoxia-stimulated cell lines [47], our results revealed that the proportion of GCs in G2/M phase was actually reduced following the $CoCl_2$ exposure. By determining the proteins that are essential for G1/S progression, we further confirmed a potential induction of G1/S checkpoint in GCs during hypoxic stimulation. To our knowledge, this study might provide the first evidence demonstrating that $CoCl_2$-mimicked hypoxia inhibits cell cycle progression in porcine GCs by blocking the G1/S transition.

HIF-1α is a major mediator of hypoxic response in mammalian tissues [48]. Although significant advances have been made towards understanding the precise mechanisms of HIF-1α action in hypoxia, the role of the porcine HIF-1α in adjusting GCs to hypoxic conditions in the follicular microenvironment remains unknown. In the present study, we generated a chemical hypoxia in porcine GCs by using $CoCl_2$, an agent that has been widely used to mimic the hypoxic conditions [49, 50]. In fact, $CoCl_2$ functions in stabilizing HIF-1α and facilitating its intracellular accumulation [50]. Here, we found that the accumulation of HIF-1α induced by $CoCl_2$ treatment was associated with the increased proportion of G1/S-arrested GCs. In contrast, HIF-1α inhibition in GCs simultaneously prevented $CoCl_2$-induced G0/G1 arrest, and restored the population in S phase. Therefore, these data first demonstrate that HIF-1α is required for suppression of G1/S transition in response to $CoCl_2$-induced hypoxia in porcine GCs.

In addition, we found that HIF-1α induces the G1/S cell cycle arrest in GCs with a FOXO1-dependent manner. $CoCl_2$ treatment led to accumulation of HIF-1α and increased FOXO1 activity as reflected by elevated expression, decreased phosphorylation, and

increased nuclear translocation. Using HIF-1α inhibitor, we showed that the induction of FOXO1 was indeed mediated by HIF-1α. These data are in agreement with an earlier report identifying FOXO1 as a potential target of HIF-1α in osteoblasts [51], whereas FOXO1 cellular localization was not detected, as also observed in our present study.

We also observed a significant increase in the expression of the CDK inhibitor Cdkn1b during $CoCl_2$ exposure, with a time course consistent with HIF-1α-induced FOXO1 activation. It has been documented that the Cdkn1b is a downstream target of the transcription factor FOXO1. In other words, FOXO1 increases the transcription of Cdkn1b [52]. As shown in our study, the inactivation of FOXO1 induced by inhibitors against the HIF-1α or FOXO1 led to the down-regulation of Cdkn1b expression, resulting in a recovery of G1/S transition in porcine GCs. Therefore, our study demonstrated, for the first time, that the induction of Cdkn1b through HIF-1α/FOXO1 is responsible for the G1/S arrest in GCs suffering $CoCl_2$-mimicked hypoxia.

Cdkn1b was first noted to bind to cyclin-CDK complexes and inhibit G1-to-S phase progression [53, 54]. Our data revealed an enhanced interaction between Cdkn1b and cyclin E/CDK2 in $CoCl_2$-treated porcine GCs. We also noticed diminished cyclin E/CDK2 activity when Cdkn1b was induced upon $CoCl_2$ stimulation. The down-regulation of Cdkn1b resulted from blocking the HIF-1α/FOXO1 pathway led to the dissociation of Cdkn1b-cyclin E/CDK2 complex, as well as a restoration of cyclin E/CDK2 activity, which might play a role in promoting S phase entry even under $CoCl_2$-mimicked hypoxia conditions. Thus, our data strongly suggest that the HIF-1α/FOXO1/Cdkn1b axis induces a G1/S arrest by modulating cyclin E/CDK2, although we cannot exclude the additional presence of a cyclin

E/CDK2-independent mechanism.

Although hypoxia inhibits cell cycle in cultured GCs, it seems to exert no apparent influence on GCs proliferation in vivo, because the multiplication of the GCs does not spontaneously stop in normally growing follicles, which were supposed to display a low oxygen internal environment during development [5, 6]. It thus raises the question whether there are certain intra-ovarian factors that might overcome the inhibitory effects of hypoxia. Insulin-like growth factor-I (IGF-I) is well recognized for its ability to increase proliferation and survival in a number of cell types [29]. In mammalian ovary, it has become evident that IGF-I regulates follicular development, for instance, by promoting proliferation and differentiation of ovarian cells [24, 29]. However, it remains elusive whether IGF-I is required for the maintenance of GCs cell cycle progression during hypoxic exposure. In the present study, the addition of IGF-I to the culture medium markedly reduced the proportion of G1/S-arrested GCs, which was accompanied by a restoration of cyclin E/CDK2 activity upon $CoCl_2$ stimulation. Conversely, blocking IGF-I function by inhibiting IGF-I receptor in $CoCl_2$-treated GCs significantly impaired the G1-to-S phase progression even in the presence of IGF-I. Therefore, these findings might provide first evidence suggesting a role of IGF-I in preventing porcine GCs from $CoCl_2$-mediated G1/S arrest.

IGF-I has been reported to regulate the growth and differentiation of GCs by activating several downstream signaling pathways, including PKA, PI3K, AKT, PKC, and ERK1/2 [30, 44, 45], although their interactions in response to hypoxia remain to be investigated in GCs. In this study, the results showed that PI3K/AKT was activated by IGF-I in porcine GCs to restore the G1/S transition upon $CoCl_2$ stimulation; whereas no definitive evidence was

observed for the involvement of PKA, PKC, and ERK1/2 in regulating cell cycle of GCs with IGF-I treatment. Previous studies indicated that FOXO1, the major downstream effector of PI3K/AKT, is phosphorylated and deactivated after exposure to IGF-I in GCs [29]. Here, we found that IGF-I-stimulated activation of PI3K/AKT in porcine GCs induced the phosphorylation of FOXO1 and the resultant nuclear exclusion of phospho-FoxO1 following $CoCl_2$-triggered G1/S arrest. In contrast, LY294002 (PI3K/AKT inhibitor) diminished IGF-I-induced G1/S transition in cultured GCs that was accompanied by down-regulation of FOXO1 activity. Correspondingly, inhibition of the PI3K/AKT pathway in GCs abolished the actions of IGF-I on suppressing Cdkn1b and its interaction with cyclin E/CDK2. Further experiments using antagonists against PI3K/AKT and/or FOXO1 showed that the suppression of FOXO1/Cdkn1b cascade through PI3K/AKT stimulated the activation of cyclin E/CDK2 complex, which in turn promoted G1-to-S phase progression in $CoCl_2$-treated GCs. Collectively, this work might provide the first evidence linking the IGF-I/PI3K/AKT/FOXO1/Cdkn1b axis to GC cell cycle regulation during $CoCl_2$-mimicked hypoxic exposure (Fig 8).

In the present study, only medium sized follicles (3-5 mm) were included. As follicles grow beyond this stage, hypoxia might become more apparent and other mechanisms could also play a role. How do larger follicles overcome the influence of hypoxia remains to be investigated in future studies. In fact, evidence has been emerged that HIF-1α in GCs might be involved in the development of antral follicles via activating expression of downstream genes, especially VEGFA, a critical agiogenic factor that facilitates vascularization in the follicle [55-57]. Therefore, it is presumable that the growing number of follicular blood

vessels might increase the oxygen supply in larger follicles, and thereby preventing hypoxia-induced cell cycle arrest in GCs.

In summary, this study provided first evidence suggesting that $CoCl_2$-mimicked hypoxia induced G1/S arrest in porcine GCs. In addition, we demonstrated that the inhibitory effects of $CoCl_2$ on GCs cell cycle are mediated through HIF-1α/FOXO1/Cdkn1b pathway. Moreover, we identified a potential role for IGF-I in maintaining G1/S transition of $CoCl_2$-treated GCs via activating the cyclin E/CDK2 complex through the PI3K/AKT/FOXO1/Cdkn1b axis. These findings not only deeply clarify the regulatory mechanism of GCs cell cycle upon hypoxic exposure, but also improve the understanding about how follicles develop under hypoxic environment in the ovary.

Competing interests

No potential conflicts of financial interests were declared.

Acknowledgements

We thank Professor Shao-chen Sun at Nanjing Agricultural University for his help and assistance in manuscript preparation and submission.

Funding

This work was supported by the National Natural Science Foundation of China (No. 31630072; No. 31601939), Program for the Top Young Talents in College of Animal Science and Technology at Nanjing Agricultural University (No. DKQB201903), the Fundamental

Research Funds for the Central Universities (No. KJQN201705), Natural Science Foundation of Jiangsu Province (No. BK20150664).

References

1. Fadhillah, Yoshioka S, Nishimura R, Okuda K. Hypoxia promotes progesterone synthesis during luteinization in bovine granulosa cells. J Reprod Dev 2014; 60:194-201.
2. Redmer DA, Reynolds LP. Angiogenesis in the ovary. Rev Reprod 1996; 1:182-192.
3. Suzuki T, Sasano H, Takaya R, Fukaya T, Yajima A, Nagura H. Cyclic changes of vasculature and vascular phenotypes in normal human ovaries. Hum Reprod 1998; 13:953-959.
4. Bianco F, Basini G, Santini S, Grasselli F. Angiogenic activity of swine granulosa cells: effects of hypoxia and the role of VEGF. Vet Res Commun 2005; 29 Suppl 2:157-159.
5. Basini G, Bianco F, Grasselli F, Tirelli M, Bussolati S, Tamanini C. The effects of reduced oxygen tension on swine granulosa cell. Regul Pept 2004; 120:69-75.
6. Neeman M, Abramovitch R, Schiffenbauer YS, Tempel C. Regulation of angiogenesis by hypoxic stress: from solid tumours to the ovarian follicle. Int J Exp Pathol 1997; 78:57-70.
7. Redding GP, Bronlund JE, Hart AL. Mathematical modelling of oxygen transport-limited follicle growth. Reproduction 2007; 133:1095-1106.
8. Greijer AE, Delis-van Diemen PM, Fijneman RJ, Giles RH, Voest EE, van Hinsbergh VW, Meijer GA. Presence of HIF-1 and related genes in normal mucosa, adenomas and carcinomas of the colorectum. Virchows Arch 2008; 452:535-544.
9. Sharp FR, Bernaudin M. HIF1 and oxygen sensing in the brain. Nat Rev Neurosci 2004; 5:437-448.
10. Iyer NV, Leung SW, Semenza GL. The human hypoxia-inducible factor 1alpha gene: HIF1A structure and evolutionary conservation. Genomics 1998; 52:159-165.
11. Ivan M, Kondo K, Yang H, Kim W, Valiando J, Ohh M, Salic A, Asara JM, Lane WS, Kaelin WG, Jr. HIFalpha targeted for VHL-mediated destruction by proline hydroxylation: implications for O2 sensing. Science 2001; 292:464-468.
12. Jaakkola P, Mole DR, Tian YM, Wilson MI, Gielbert J, Gaskell SJ, von Kriegsheim A, Hebestreit HF, Mukherji M, Schofield CJ, Maxwell PH, Pugh CW, et al. Targeting of HIF-alpha to the von Hippel-Lindau ubiquitylation complex by O2-regulated prolyl hydroxylation. Science 2001; 292:468-472.
13. Masson N, Willam C, Maxwell PH, Pugh CW, Ratcliffe PJ. Independent function of two destruction domains in hypoxia-inducible factor-alpha chains activated by prolyl hydroxylation. EMBO J 2001; 20:5197-5206.
14. Harris AL. Hypoxia--a key regulatory factor in tumour growth. Nat Rev Cancer 2002; 2:38-47.
15. Duncan WC, van den Driesche S, Fraser HM. Inhibition of vascular endothelial growth factor in the primate ovary up-regulates hypoxia-inducible factor-1alpha in the follicle and corpus luteum. Endocrinology 2008; 149:3313-3320.
16. Kim J, Bagchi IC, Bagchi MK. Signaling by hypoxia-inducible factors is critical for ovulation in mice. Endocrinology 2009; 150:3392-3400.
17. Ortmann B, Druker J, Rocha S. Cell cycle progression in response to oxygen levels. Cell Mol Life Sci

2014; 71:3569-3582.
18. Gardner LB, Li Q, Park MS, Flanagan WM, Semenza GL, Dang CV. Hypoxia inhibits G1/S transition through regulation of p27 expression. J Biol Chem 2001; 276:7919-7926.
19. Huang L, Ao Q, Zhang Q, Yang X, Xing H, Li F, Chen G, Zhou J, Wang S, Xu G, Meng L, Lu Y, et al. Hypoxia induced paclitaxel resistance in human ovarian cancers via hypoxia-inducible factor 1alpha. J Cancer Res Clin Oncol 2010; 136:447-456.
20. Krtolica A, Krucher NA, Ludlow JW. Hypoxia-induced pRB hypophosphorylation results from downregulation of CDK and upregulation of PP1 activities. Oncogene 1998; 17:2295-2304.
21. Green SL, Freiberg RA, Giaccia AJ. p21(Cip1) and p27(Kip1) regulate cell cycle reentry after hypoxic stress but are not necessary for hypoxia-induced arrest. Mol Cell Biol 2001; 21:1196-1206.
22. Krtolica A, Krucher NA, Ludlow JW. Molecular analysis of selected cell cycle regulatory proteins during aerobic and hypoxic maintenance of human ovarian carcinoma cells. Br J Cancer 1999; 80:1875-1883.
23. Baddela VS, Sharma A, Viergutz T, Koczan D, Vanselow J. Low Oxygen Levels Induce Early Luteinization Associated Changes in Bovine Granulosa Cells. Front Physiol 2018; 9:1066.
24. Yoshimura Y, Ando M, Nagamatsu S, Iwashita M, Adachi T, Sueoka K, Miyazaki T, Kuji N, Tanaka M. Effects of insulin-like growth factor-I on follicle growth, oocyte maturation, and ovarian steroidogenesis and plasminogen activator activity in the rabbit. Biol Reprod 1996; 55:152-160.
25. Zhou J, Chin E, Bondy C. Cellular pattern of insulin-like growth factor-I (IGF-I) and IGF-I receptor gene expression in the developing and mature ovarian follicle. Endocrinology 1991; 129:3281-3288.
26. Bryan KA, Hammond JM, Canning S, Mondschein J, Carbaugh DE, Clark AM, Hagen DR. Reproductive and growth responses of gilts to exogenous porcine pituitary growth hormone. J Anim Sci 1989; 67:196-205.
27. Oliver JE, Aitman TJ, Powell JF, Wilson CA, Clayton RN. Insulin-like growth factor I gene expression in the rat ovary is confined to the granulosa cells of developing follicles. Endocrinology 1989; 124:2671-2679.
28. Adashi EY, Resnick CE, Rosenfeld RG. Insulin-like growth factor-I (IGF-I) and IGF-II hormonal action in cultured rat granulosa cells: mediation via type I but not type II IGF receptors. Endocrinology 1990; 126:216-222.
29. Quirk SM, Cowan RG, Harman RM, Hu CL, Porter DA. Ovarian follicular growth and atresia: the relationship between cell proliferation and survival. J Anim Sci 2004; 82 E-Suppl:E40-52.
30. Hu CL, Cowan RG, Harman RM, Quirk SM. Cell cycle progression and activation of Akt kinase are required for insulin-like growth factor I-mediated suppression of apoptosis in granulosa cells. Mol Endocrinol 2004; 18:326-338.
31. Kadakia R, Arraztoa JA, Bondy C, Zhou J. Granulosa cell proliferation is impaired in the Igf1 null ovary. Growth Horm IGF Res 2001; 11:220-224.
32. Huang H, Tindall DJ. Dynamic FoxO transcription factors. J Cell Sci 2007; 120:2479-2487.
33. Burgering BM, Kops GJ. Cell cycle and death control: long live Forkheads. Trends Biochem Sci 2002; 27:352-360.
34. Chu CY, Jin YT, Zhang W, Yu J, Yang HP, Wang HY, Zhang ZJ, Liu XP, Zou Q. CA IX is upregulated in CoCl2-induced hypoxia and associated with cell invasive potential and a poor prognosis of breast cancer. Int J Oncol 2016; 48:271-280.
35. Dai ZJ, Gao J, Ma XB, Yan K, Liu XX, Kang HF, Ji ZZ, Guan HT, Wang XJ. Up-regulation of hypoxia inducible factor-1alpha by cobalt chloride correlates with proliferation and apoptosis in PC-2 cells. J

Exp Clin Cancer Res 2012; 31:28.
36. Yuan Y, Hilliard G, Ferguson T, Millhorn DE. Cobalt inhibits the interaction between hypoxia-inducible factor-alpha and von Hippel-Lindau protein by direct binding to hypoxia-inducible factor-alpha. J Biol Chem 2003; 278:15911-15916.
37. Vengellur A, LaPres JJ. The role of hypoxia inducible factor 1alpha in cobalt chloride induced cell death in mouse embryonic fibroblasts. Toxicol Sci 2004; 82:638-646.
38. Koh MY, Spivak-Kroizman T, Venturini S, Welsh S, Williams RR, Kirkpatrick DL, Powis G. Molecular mechanisms for the activity of PX-478, an antitumor inhibitor of the hypoxia-inducible factor-1alpha. Mol Cancer Ther 2008; 7:90-100.
39. Shen M, Liu Z, Li B, Teng Y, Zhang J, Tang Y, Sun SC, Liu H. Involvement of FoxO1 in the effects of follicle-stimulating hormone on inhibition of apoptosis in mouse granulosa cells. Cell Death Dis 2014; 5:e1475.
40. Shen M, Jiang Y, Guan Z, Cao Y, Li L, Liu H, Sun SC. Protective mechanism of FSH against oxidative damage in mouse ovarian granulosa cells by repressing autophagy. Autophagy 2017; 13:1364-1385.
41. Geisen C, Moroy T. The oncogenic activity of cyclin E is not confined to Cdk2 activation alone but relies on several other, distinct functions of the protein. J Biol Chem 2002; 277:39909-39918.
42. Goldenberg RL, Vaitukaitis JL, Ross GT. Estrogen and follicle stimulation hormone interactions on follicle growth in rats. Endocrinology 1972; 90:1492-1498.
43. Gong JG, McBride D, Bramley TA, Webb R. Effects of recombinant bovine somatotrophin, insulin-like growth factor-I and insulin on the proliferation of bovine granulosa cells in vitro. J Endocrinol 1993; 139:67-75.
44. Makarevich A, Sirotkin A, Chrenek P, Bulla J, Hetenyi L. The role of IGF-I, cAMP/protein kinase A and MAP-kinase in the control of steroid secretion, cyclic nucleotide production, granulosa cell proliferation and preimplantation embryo development in rabbits. J Steroid Biochem Mol Biol 2000; 73:123-133.
45. He H, Herington AC, Roupas P. Effects of phorbol ester and staurosporine on the actions of insulin-like growth factor-I on rat ovarian granulosa cells. Endocrine 1995; 3:159-167.
46. Robker RL, Richards JS. Hormone-induced proliferation and differentiation of granulosa cells: a coordinated balance of the cell cycle regulators cyclin D2 and p27Kip1. Mol Endocrinol 1998; 12:924-940.
47. Green SL, Giaccia AJ. Tumor hypoxia and the cell cycle: implications for malignant progression and response to therapy. Cancer J Sci Am 1998; 4:218-223.
48. Adams JM, Difazio LT, Rolandelli RH, Lujan JJ, Hasko G, Csoka B, Selmeczy Z, Nemeth ZH. HIF-1: a key mediator in hypoxia. Acta Physiol Hung 2009; 96:19-28.
49. Ciafre SA, Niola F, Giorda E, Farace MG, Caporossi D. CoCl(2)-simulated hypoxia in skeletal muscle cell lines: Role of free radicals in gene up-regulation and induction of apoptosis. Free Radic Res 2007; 41:391-401.
50. Piret JP, Mottet D, Raes M, Michiels C. CoCl2, a chemical inducer of hypoxia-inducible factor-1, and hypoxia reduce apoptotic cell death in hepatoma cell line HepG2. Ann N Y Acad Sci 2002; 973:443-447.
51. Xu G. HIF-1-mediated expression of Foxo1 serves an important role in the proliferation and apoptosis of osteoblasts derived from children's iliac cancellous bone. Mol Med Rep 2018; 17:6621-6631.
52. Schmidt M, Fernandez de Mattos S, van der Horst A, Klompmaker R, Kops GJ, Lam EW, Burgering BM, Medema RH. Cell cycle inhibition by FoxO forkhead transcription factors involves

downregulation of cyclin D. Mol Cell Biol 2002; 22:7842-7852.
53. Liang J, Zubovitz J, Petrocelli T, Kotchetkov R, Connor MK, Han K, Lee JH, Ciarallo S, Catzavelos C, Beniston R, Franssen E, Slingerland JM. PKB/Akt phosphorylates p27, impairs nuclear import of p27 and opposes p27-mediated G1 arrest. Nat Med 2002; 8:1153-1160.
54. Ciarallo S, Subramaniam V, Hung W, Lee JH, Kotchetkov R, Sandhu C, Milic A, Slingerland JM. Altered p27(Kip1) phosphorylation, localization, and function in human epithelial cells resistant to transforming growth factor beta-mediated G(1) arrest. Mol Cell Biol 2002; 22:2993-3002.
55. Alam H, Maizels ET, Park Y, Ghaey S, Feiger ZJ, Chandel NS, Hunzicker-Dunn M. Follicle-stimulating hormone activation of hypoxia-inducible factor-1 by the phosphatidylinositol 3-kinase/AKT/Ras homolog enriched in brain (Rheb)/mammalian target of rapamycin (mTOR) pathway is necessary for induction of select protein markers of follicular differentiation. J Biol Chem 2004; 279:19431-19440.
56. Alam H, Weck J, Maizels E, Park Y, Lee EJ, Ashcroft M, Hunzicker-Dunn M. Role of the phosphatidylinositol-3-kinase and extracellular regulated kinase pathways in the induction of hypoxia-inducible factor (HIF)-1 activity and the HIF-1 target vascular endothelial growth factor in ovarian granulosa cells in response to follicle-stimulating hormone. Endocrinology 2009; 150:915-928.
57. Thompson JG, Brown HM, Kind KL, Russell DL. The Ovarian Antral Follicle: Living on the Edge of Hypoxia or Not? Biol Reprod 2015; 92:153.

Figure Legends

Fig. 1. $CoCl_2$-induced hypoxia causes a cell cycle arrest in porcine GCs. (A) Western blot analysis of HIF-1α level in porcine GCs treated with $CoCl_2$ (100 μM). The protein level of HIF-1α was up-regulated by $CoCl_2$. The protein bands were quantified densitometrically using ImageJ 1.42q software. (B) Porcine GCs were cultured in medium containing 100 μM $CoCl_2$ for 24 h, and then collected for cell cycle analysis using flow cytometry. The cell cycle of GCs was quantified using the ModFit LT 3.2 software. (C) Proteins levels of CDK2, CDK4, CDK6, cyclin D1, cyclin E1, and Cdkn1b were determined by western blot. The protein bands were quantified densitometrically using ImageJ 1.42q software. (D) Laser

confocal-scanning microscopy was employed to observe the protein level of Cdkn1b by immunofluorescence assay, Bar, 10 μm. The optical density of Cdkn1b staining was quantified using ImageJ 1.42q software. Experiments were repeated in triplicate, and three fields of each coverslip were selected in random for counting. Data represent mean ± S.E; n = 3. *P < 0.05. (E) After 6 h of $CoCl_2$ (100 μM) incubation, the activity of CDK2/CyclinE1 was measured in cultured GCs. The numbers on the Y axis represent the activity unit (μ mol NADH/min) of CDK1/cyclin E complex. Corresponding data represent mean ± S.E; n = 3. *P < 0.05, **P < 0.01; ***P < 0.001.

Fig. 2. $CoCl_2$-stimulated HIF-1α prevents porcine GCs from G1/S transition. (A) Porcine GCs were cultured for 2 h in medium containing different concentrations of PX-478, a specific inhibitor of HIF-1α, treated with 100 μM $CoCl_2$ for 24 h, and then collected for cell cycle analysis using flow cytometry. The cell cycle distribution of GCs was quantified using the ModFit LT 3.2 software. (B) The quantification diagram of GCs cell cycle distribution. * represent P < 0.05, ** represent P < 0.01; *** represent P < 0.001. (C) Western blot analysos of cell cycle-related proteins and HIF-1α in GCs with the indicated treatments. The protein bands were quantified densitometrically using ImageJ 1.42q software. (D) Porcine GCs were cultured in medium containing 100 μM $CoCl_2$ and 30 μM IGF-I for 6 h. Laser confocal-scanning microscopy was employed to observe the protein level of Cdkn1b visualized by immunofluorescence staining, Bar, 10 μM. The optical density of Cdkn1b staining was quantified using ImageJ 1.42q software. Experiments were repeated in triplicate, and three fields of each coverslip were selected in random for counting. Data represent mean

± S.E; n = 3. *P < 0.05. (E) Porcine GCs pretreated with PX-478 (2 μM) for 2 h, then were incubated with $CoCl_2$ (100 μM) for 6 h, and the activity of CDK2/CyclinE1 was then determined in cultured GCs. Corresponding data represent mean ± S.E; n = 3. *P < 0.05, **P < 0.01; ***P < 0.001.

Fig. 3. HIF-1α activates FOXO1 activity to inhibit cyclin E/CDK2 activity. (A) Western blot analysis of FOXO1 and p-FOXO1 (Ser256) level in porcine GCs treated with $CoCl_2$ (100 μM). The protein level of FOXO1 was up-regulated and p-FOXO1(Ser256) was down-regulated in a time-dependent manner when porcine GCs were treated with 100 μM $CoCl_2$. (B) Western blot detection of the corresponding p-AKT (Ser473) levels, which was down-regulated in a time-dependent manner after 100 μM $CoCl_2$ treatment. (C) Porcine GCs were pretreated with PX-478 (2 μM) for 2 h, incubated with $CoCl_2$ (100 μM) for 6 h, and the proteins level of p-AKT (Ser473), AKT, p-mTOR (Ser2448), mTOR, p-FOXO1 (Ser256), and FOXO1 were then determined by western blot. The protein bands were quantified densitometrically using ImageJ 1.42q software.

Fig. 4. Inhibition of cyclin E/CDK2 activity through the HIF-1α/FOXO1/Cdkn1b axis is required for the induction of G1/S arrest. (A) Porcine GCs were cultured in medium containing 2 μM PX-478 for 2 h, treated with 100 μM $CoCl_2$ for 6 h, and then collected to observe the subcellular localization of of FOXO1 by immunofluorescence assay. Bar, 10 μM. The lower panel indicates the percentage of cells with FOXO1 in the nucleus (orange bars) and in the cytosol (green bars). Experiments were performed in triplicate, and cells were

counted in three randomly selected fields in each coverslip. Arrows indicate cells with nuclear FOXO1. Data represent mean ± S.E; n = 3. ***P < 0.001. (B) GCs pretreatment with 500 nM AS1842856,a specific inhibitor of FOXO1 for 2 h, were then incubated with $CoCl_2$ (100 μM) for 6 h. The protein level of Cdkn1b was analysed by immunofluorescence assay. Bar, 10 μM. The optical density of Cdkn1b staining was quantified using ImageJ 1.42q software. Experiments were repeated in triplicate, and three fields of each coverslip were selected in random for counting. Data represent mean ± S.E; n = 3. *P < 0.05, **P < 0.01. (C) The corresponding proteins level of Cdkn1b, p-FOXO1 (Ser256), FOXO1, p-AKT (Ser473), AKT were determined by western blot. The protein bands were quantified densitometrically using ImageJ 1.42q software. (D) After treatment with $CoCl_2$ (100 μM) for 6 h, the interaction of Cdkn1b and CDK2/Cyclin E1 was determined by immunoprecipitation assay. The protein bands were quantified densitometrically using ImageJ 1.42q software. WCL, whole cell lysates. (E) Porcine GCs were pretreated with 500 nM AS1842856 and 2 μM PX-478 for 2 h, cultured with $CoCl_2$ (100 μM) for 6 h, the interaction of Cdkn1b and CDK2/Cyclin E1 was then determined by immunoprecipitation assay. The protein bands were quantified densitometrically using ImageJ 1.42q software. (F) Porcine GCs were pretreated with 500 nM AS1842856 and 2 μM PX-478 for 2 h, treated with $CoCl_2$ (100 μM) for 6 h, and then collected for cell cycle analysis using flow cytometry. The cell cycle distribution of GCs was quantified using the ModFit LT 3.2 software. (G) The activity of CDK2/Cyclin E1 was determined in cells with the indicated treatments. Corresponding data represent mean ± S.E; n = 3. *P < 0.05, **P < 0.01; ***P < 0.001; NS, not significant, P > 0.05.

Fig. 5. IGF-I restore G1/S transition in $CoCl_2$-treated porcine GC. (A) Porcine GCs were treated with $CoCl_2$ (100 μM) and IGF-I (30 nM) for 24 h, then collected for cell cycle analysis using flow cytometry. The G0/G1 (B), S (C), G2/M (D) proportion of GCs was quantified using the ModFit LT 3.2 software. (E) The activity of CDK2/Cyclin E1 was determined in GCs treated as above. Corresponding data represent mean ± S.E; n = 3. *P < 0.05, **P < 0.01; ***P < 0.001; NS, not significant, P > 0.05.

Fig. 6. IGF-I overcomes $CoCl_2$-induced G1/S arrest via activating the PI3K/AKT signaling. (A) GCs pretreated for 2 h with 10 μM LY294002 (a inhibitor of PI3K/AKT pathway) were then incubated with $CoCl_2$ (100 μM) and IGF-I (30 nM) for 24 h. Cells were then collected for cell cycle analysis using flow cytometry. The G0/G1 (B), S (C), G2/M (D) proportion of GCs was quantified using the ModFit LT 3.2 software. **(E-H)** The activity of CDK2/Cyclin E1 was determined in porcine GCs treated with $CoCl_2$ (100 μM) and IGF-I (30 nM) for 6 h. PKA inhibitor H89 (5 μM) (E), PI3K/AKT inhibitor LY294002 (10 μM) (F), PKC inhibitor Go6983 (5 μM) (G), or ERK1/2 inhibitor SCH772984 (1 μM) (H) were added 2 h before $CoCl_2$ incubation. Corresponding data represent mean ± S.E; n = 3. *P < 0.05, **P < 0.01; ***P < 0.001; NS, not significant, P > 0.05.

Fig. 7. The effects of IGF-I are mediated by activating cyclin E/CDK2 through the PI3K/AKT/FOXO1/Cdkn1b axis. (A) Porcine GCs were treated with $CoCl_2$ (100 μM) and IGF-I (30 nM) for 6 h, the proteins level of p-AKT (Ser473), AKT, p-FOXO1 (Ser256), FOXO1, Cdkn1b and HIF-1α were determined by western blot. The protein bands were

quantified densitometrically using ImageJ 1.42q software. (B) Porcine GCs pretreated with 10 μM LY294002 for 2 h were incubated with $CoCl_2$ (100 μM) and IGF-I (30 nM) for another 24 h. Cells were then collected to observe the subcellular localization of FOXO1 by immunofluorescence assay. Bar, 10 μM. (C) The corresponding change of Cdkn1b protein level was determined by immunofluorescence assay, Bar, 10 μM. (D) Western blot analysis of p-AKT (Ser473), AKT, and Cdkn1b protein level in GCs with the same treatment as mentioned above. The protein bands were quantified densitometrically using ImageJ 1.42q software. (E) The interaction between Cdkn1b and CDK2/Cyclin E1 was analysed by immunoprecipitation assay in GCs with above treatment. The protein bands were quantified densitometrically using ImageJ 1.42q software. (F) Porcine GCs pretreated with LY294002 (10 μM) and AS1842856 (500 nM) for 2 h were incubated with $CoCl_2$ (100 μM) and IGF-I (30 nM) for 6 h. Cells were then collected for determining the activity of CDK2/Cyclin E1. (G) The interaction between Cdkn1b and CDK2/Cyclin E1 was analysed by immunoprecipitation assay in GCs with above treatment. The protein bands were quantified densitometrically using ImageJ 1.42q software. (H) The cell cycle distribution was determined by flow cytometry in GCs following the indicated treatments. (I) The G0/G1, S, G2/M proportion of GCs was quantified using the ModFit LT 3.2 software. Corresponding data represent mean ± S.E; n = 3. *$P < 0.05$, **$P < 0.01$; ***$P < 0.001$; NS, not significant, $P > 0.05$.

Fig. 8. A proposed model for IGF-I-mediated cell cycle regulation in porcine GCs during hypoxic exposure. Under hypoxic conditions, HIF-1α is accumulated to induce

FOXO1 activity partly by inhibiting AKT, resulting in FOXO1 dephosphorylation and nuclear retention, which in turn transmits hypoxic signals via up-regulating the expression of Cdkn1b, an inhibitor of cyclin dependent kinase, leading to cyclin E/CDK2 deactivation and the resultant G1/S cell cycle arrest in porcine GCs. However, in the presence of IGF-I, the activation of PI3K/AKT signaling blocks the nuclear translocation of FOXO1, terminating the FOXO1-induced Cdkn1b expression, thus recovering the G1-to-S phase transition in GCs by removal of Cdkn1b-mediated cyclin E/CDK2 inhibition upon hypoxic stimulation.

Fig-1

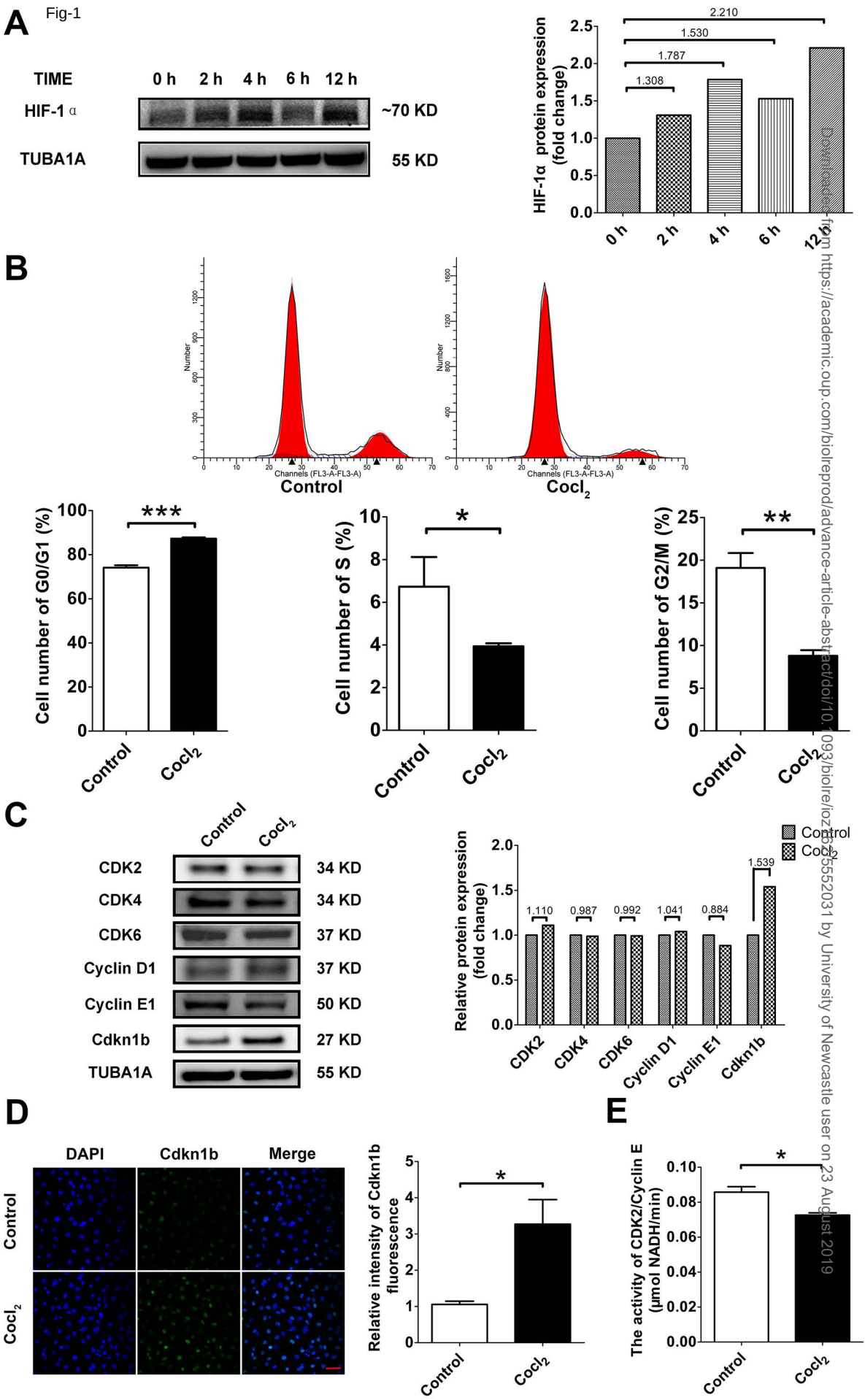

Fig-2

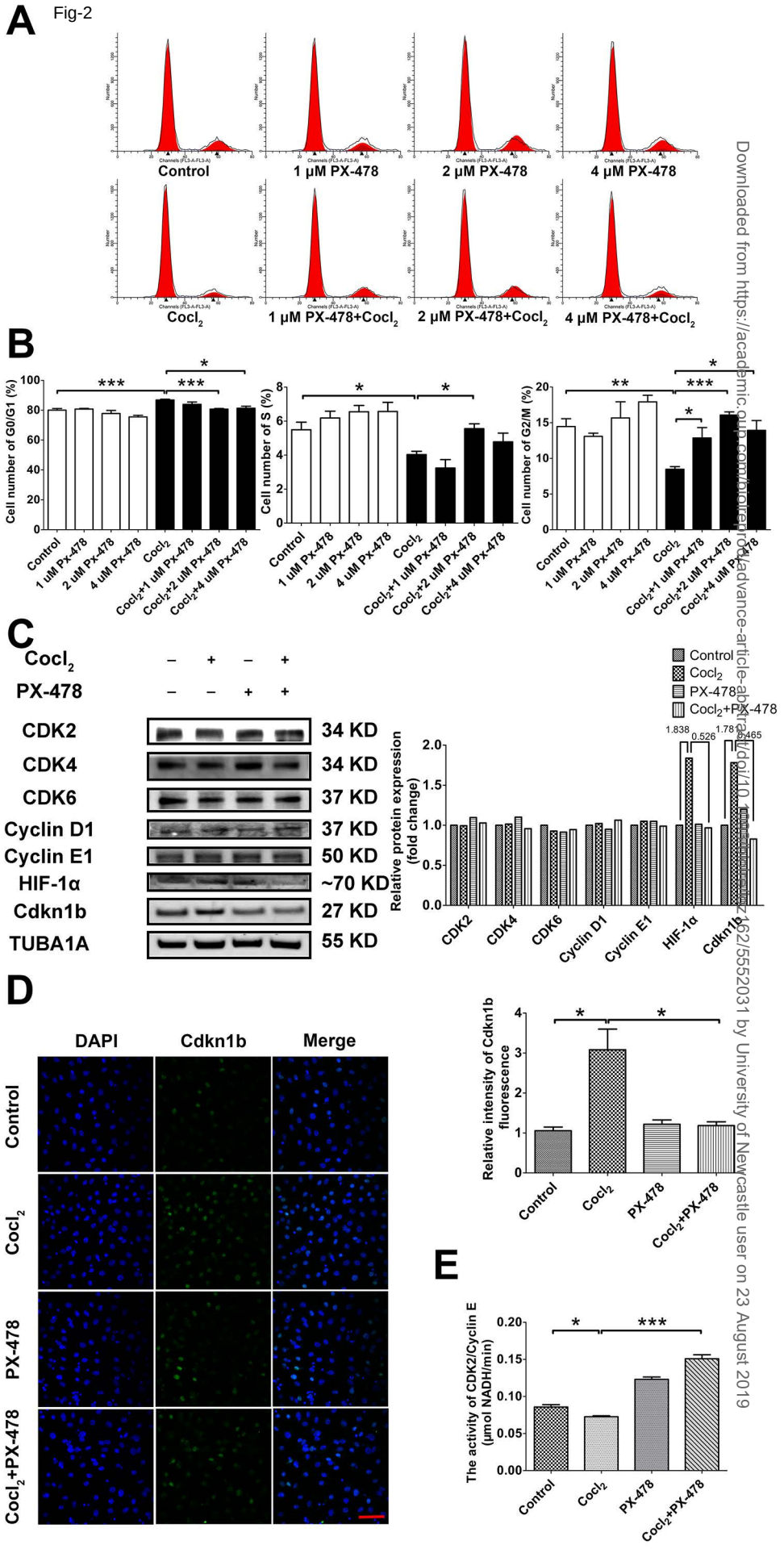

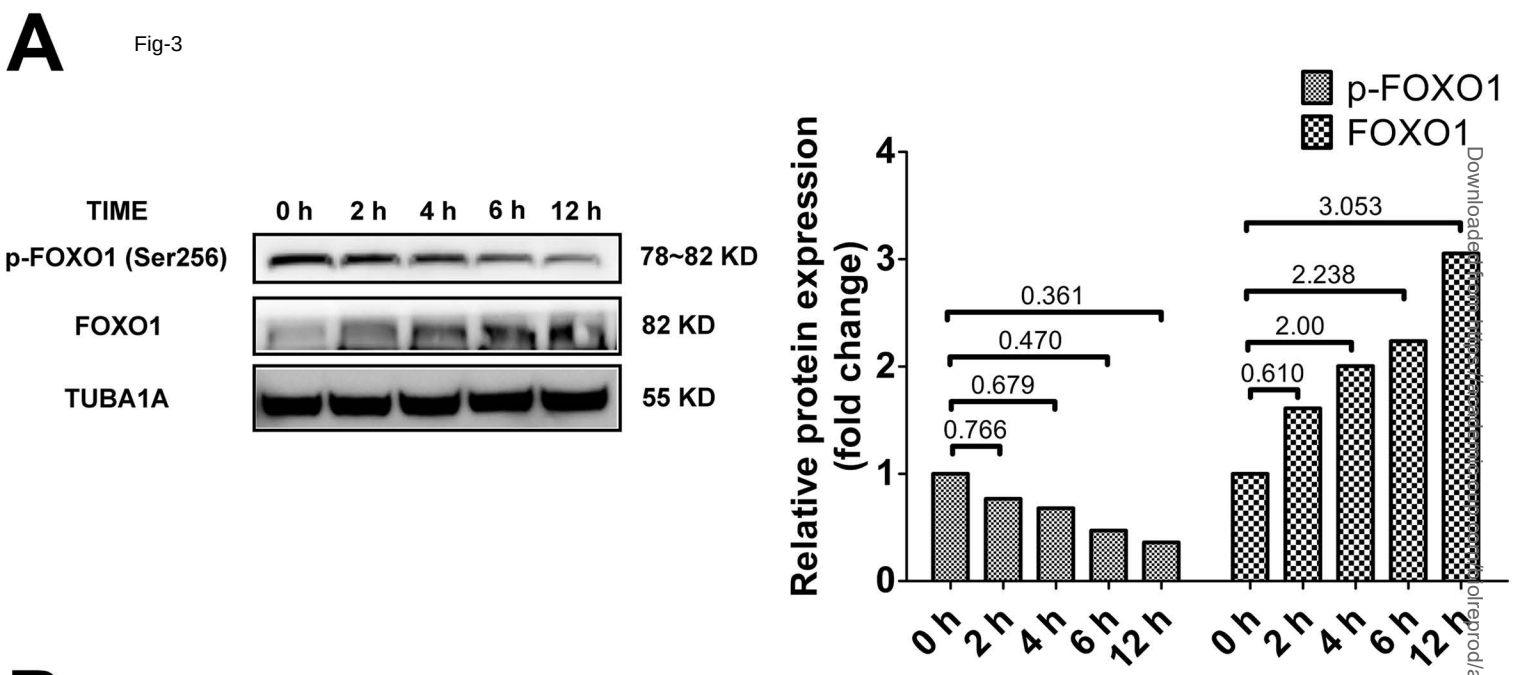

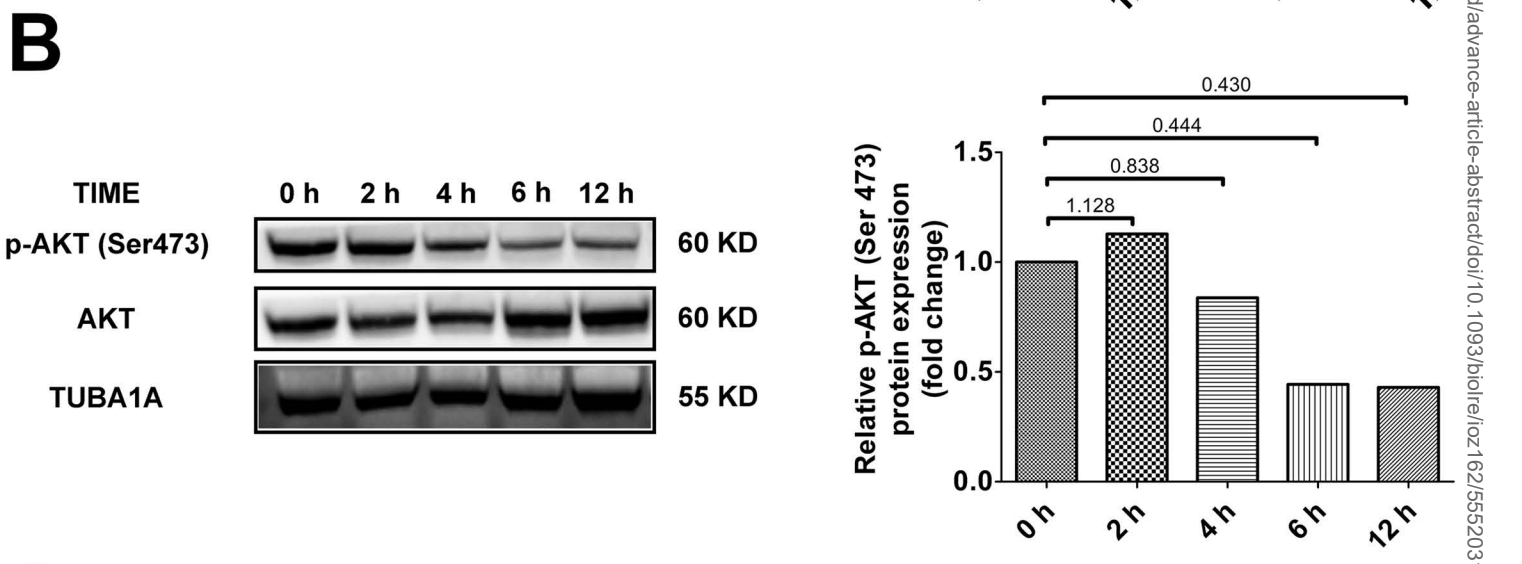

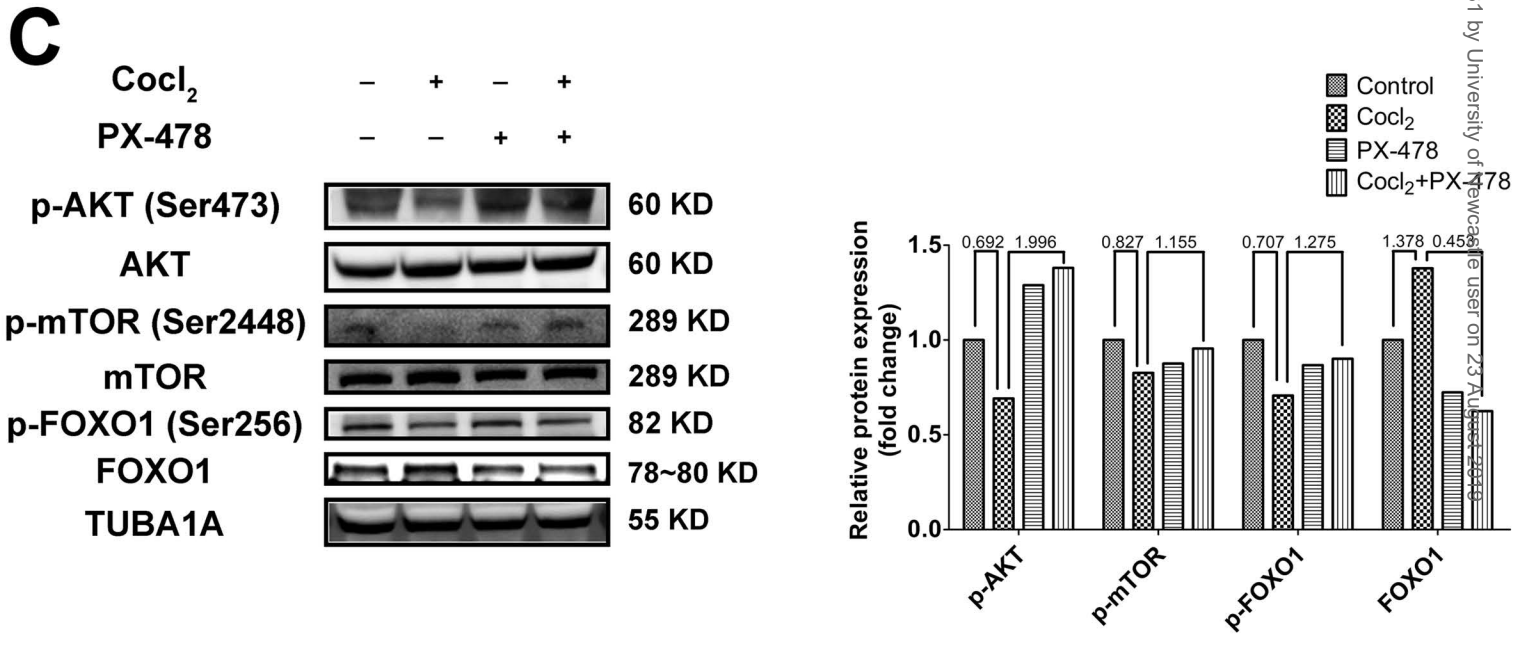

Fig-4

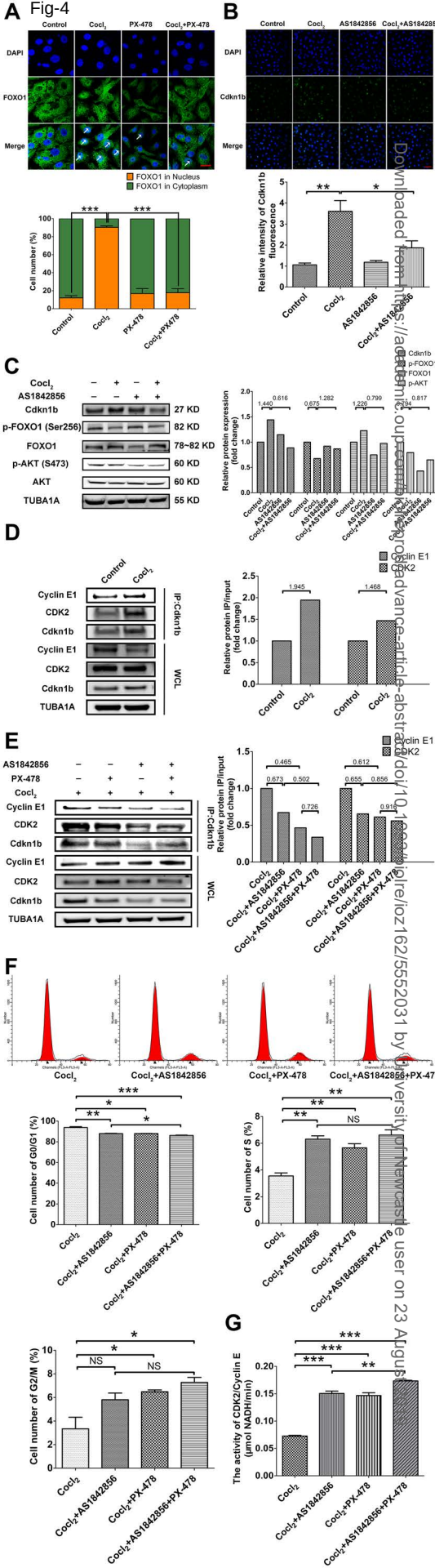

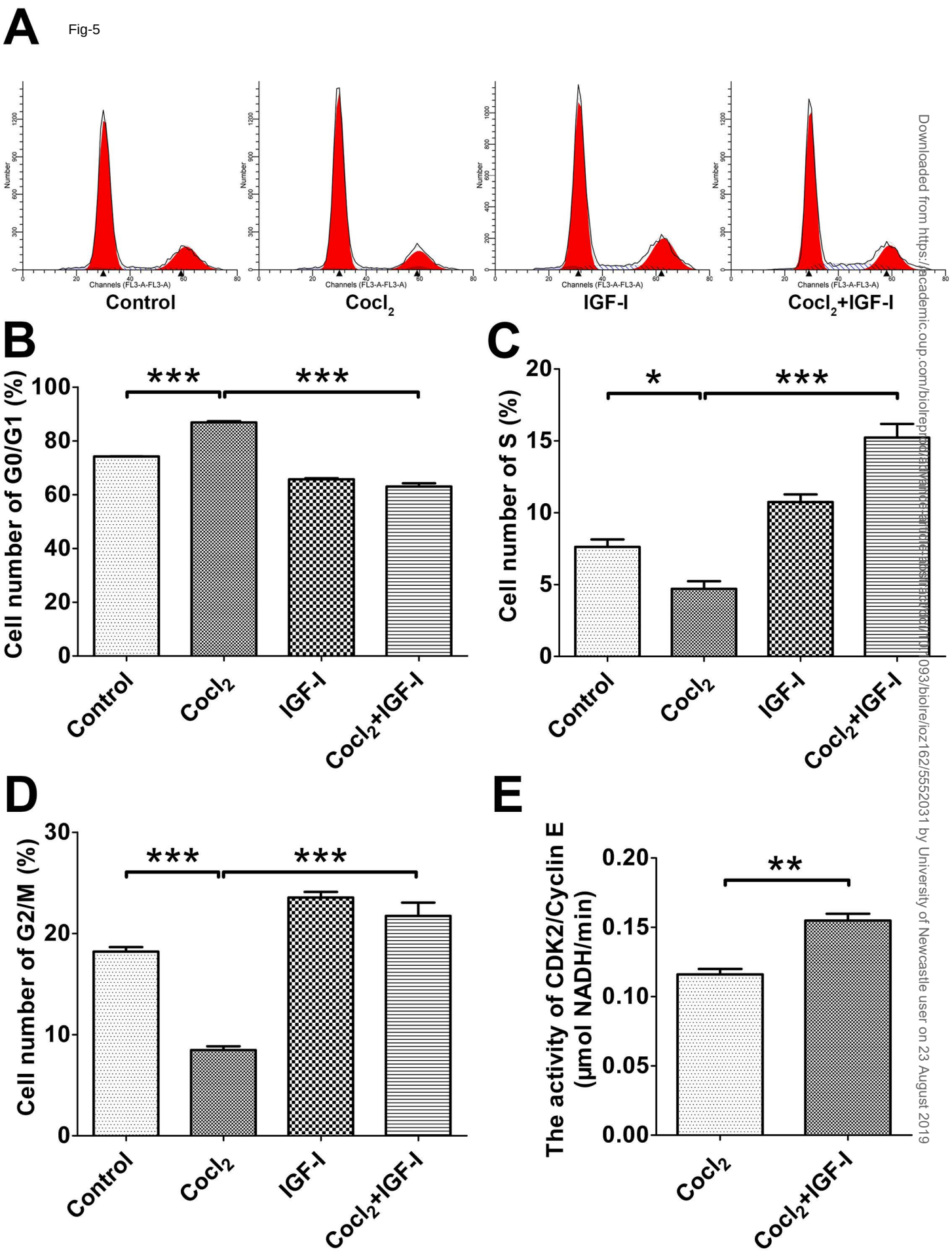

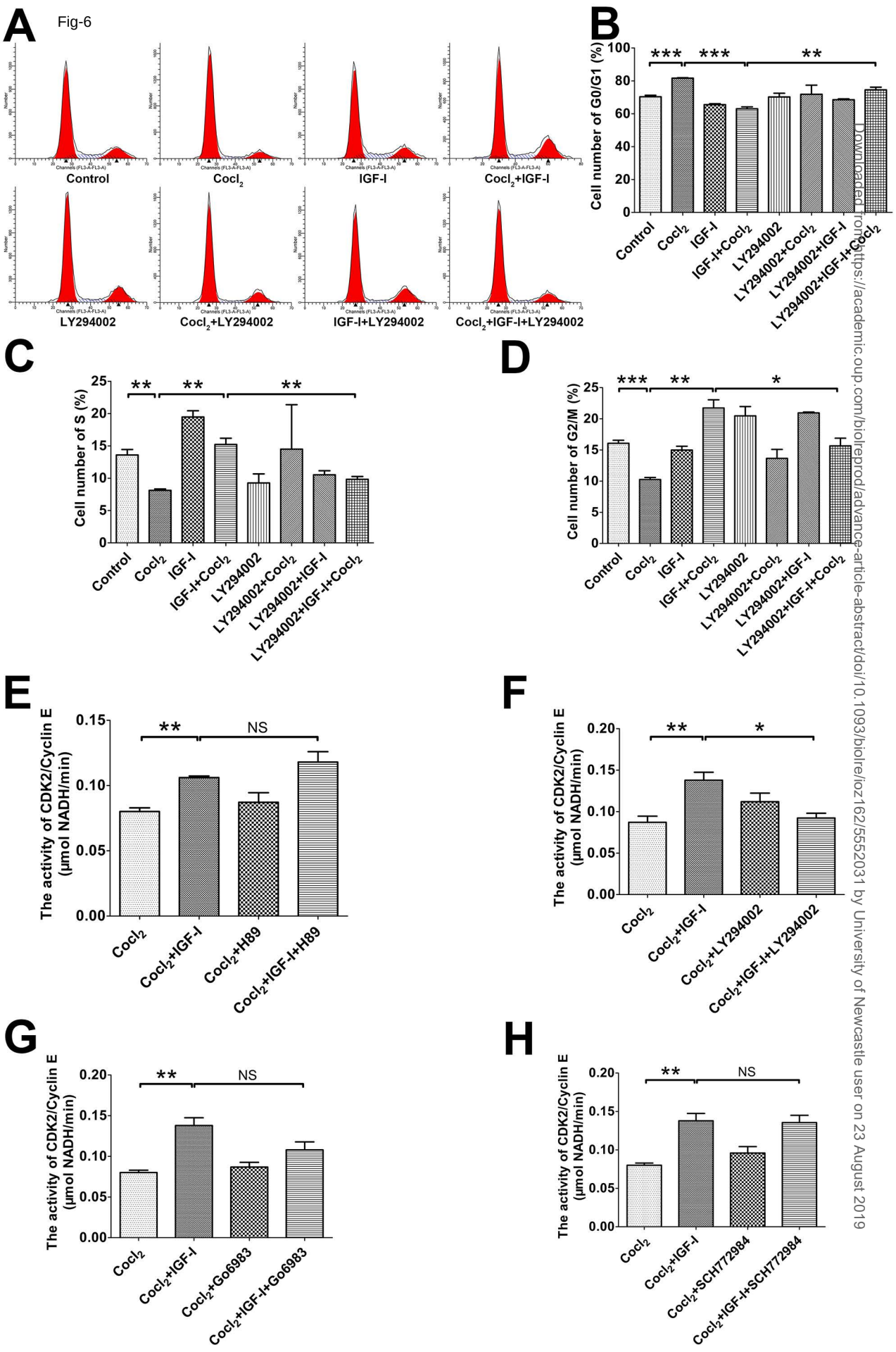

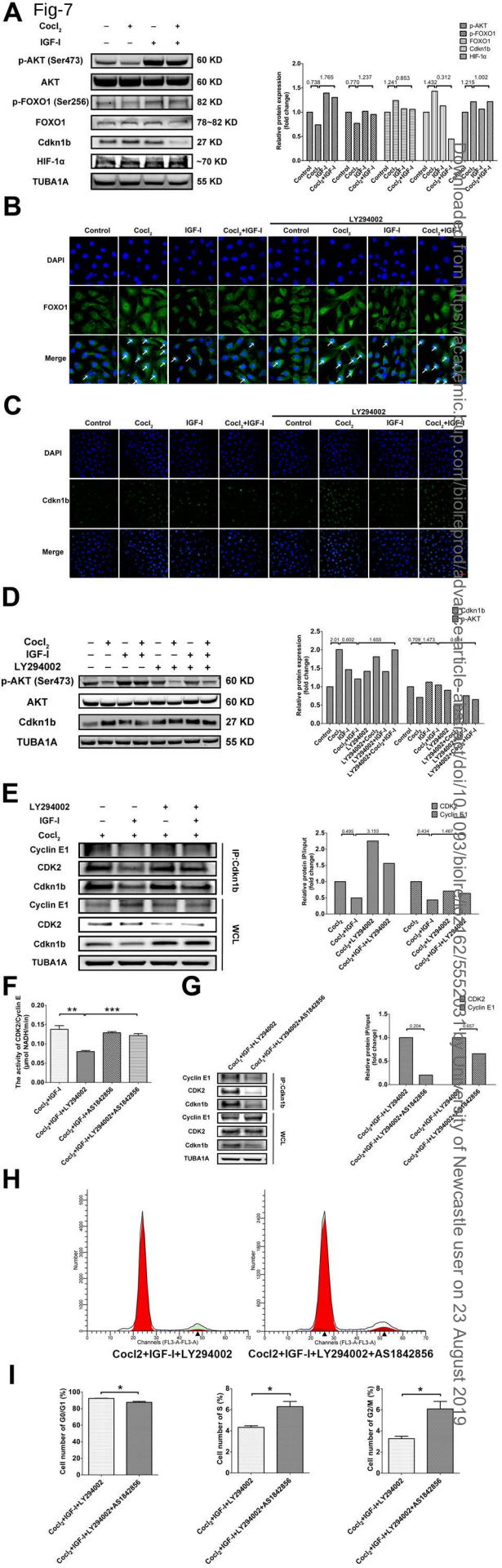

Fig-8